Mater. Res. Soc. Symp. Proc. Vol. 1659 © 2014 Materials Research Society
DOI: 10.1557/opl.2014.98

High Resolution Position Monitoring of Suspended MEMS towards Biological and Chemical Sensors

G. Putrino[1], M. Martyniuk[1], A. Keating[2], J.M. Dell[1], and L. Faraone[1]

[1]School of Electrical, Electronic and Computer Engineering, The University of Western Australia, 35 Stirling Hwy, Crawley, WA 6009, Australia

[2]School of Mechanical and Chemical Engineering, The University of Western Australia, 35 Stirling Hwy, Crawley, WA 6009, Australia

ABSTRACT

We present an integrated readout technique for interrogating the suspension height of micro-electro-mechanical systems (MEMS) structures. This readout technique is envisaged to be useful in applications such as MEMS-based biological and chemical sensing, where it is necessary to obtain the accurate position of a MEMS beam. The approach is based on the suspended MEMS structure modulating light transmission in an underlying optical waveguide via Fabry-Perrot phenomena. The performance of the technique is predicted via finite difference time domain (FDTD) simulations the results of which are confirmed by experimental measurements.

INTRODUCTION

Microcantilever sensors are readily integrated into an array using low-cost, mass-production fabrication techniques developed for micro-electro-mechanical systems (MEMS), and can facilitate simultaneous multi-analyte chemical sensing [1-3]. MEMS-based microstructures are extremely sensitive elements, demonstrating mass detection limits as low as 10^{-21} g in controlled, laboratory conditions [4, 5]. If the top surface of the micro-cantilever is functionalized to preferentially adsorb specific molecules, an extremely sensitive and selective sensor can be fabricated.

Readout technologies for MEMS sensors include the use of light reflected from the cantilever tip to a distant quadrant detector [1], electrical sensing (piezoresistive, piezoelectric, capacitive, Lorentz force/emf sensing and tunneling current techniques), and optical sensing based on optical interference either in an interferometer or the use of diffraction from an optical grating formed by a line of cantilevers. This latter configuration is often described as an array in the literature, but is still effectively a sensor for a single analyte [4, 6, 7].

The typical deflection noise density (DND) for micro-cantilever sensor systems that use quadrant detectors such as those found in atomic force microscopes (AFMs) is in the range of 100-1000 fm/√Hz, although laboratory values of 17 fm/√Hz have been achieved [8, 9]. The lowest shot noise limited DND previously reported was 6 fm/√Hz for a readout using an optical resonance approach [10]. A significant drawback of these AFM-based readout approaches is that none of them is compatible with the passive, non-electrical readout of compact, large arrays of individually and uniquely functionalized MEMS sensors. Future techniques will need to have the sensitivity of the above techniques, plus the ability to address large arrays of MEMS structures. Recently developed techniques to address large arrays include using cantilevers as optical waveguides [11], optical differential detection methods [12], or photonic microharp arrays [13].

In order to meet the requirement of the highly sensitive readout of large cantilever arrays, our investigations have focused on resonant optical interferometric techniques that lend themselves easily to large scale integration and are compatible with division multiplexed systems. In this work we will present experimental validation of the technique and compare it to finite difference time domain (FDTD) simulations of the device.

DEVICE DESCRIPTION AND MODELLING

The proposed and investigated approach is schematically shown in Fig. 1. In sensing applications, a doubly clamped beam would change its height or mechanical resonance frequency in response to an absorbed analyte. To sense such changes, an optically resonant cavity is created when a MEMS beam with a reflective undersurface is suspended above a diffraction grating etched into a waveguide. When light travels through the silicon waveguide, the grating will diffract some of the light out of the waveguide towards the MEMS beam. The MEMS beam will reflect the light back towards the grating, creating an interferometric effect. The intensity of the light travelling through the waveguide is hence amplitude modulated by movement of the MEMS beam.

Figure 1(b) shows a cross-section of the full device. Light is launched into the silicon waveguide via the input grating coupler. The grating couplers were designed to be broadband and have optimized coupling efficiency for light at a wavelength of 1550 nm [14]. The light modulated by the interferometer is coupled out by an output grating coupler providing a sensitive measure of the beam deflection.

Two dimensional electromagnetic modeling of the structure was undertaken using the Meep finite difference time domain (FDTD) package [15]. The model was based on a silicon-on-insulator (SOI) platform for the optical waveguide/grating structure, which consisted of a 230 nm epitaxial silicon layer for the waveguide, 2000 nm thick buried oxide for the bottom cladding layer, and a silicon handle wafer as the base. The waveguides are designed to be single mode in the direction perpendicular to the plane of the substrate and multimode in the plane of the waveguide. SOI photonic structures have the advantage of being a relatively well developed technology. Further, silicon provides very strong optical guiding so that minimal evanescent field coupling will occur, reducing crosstalk and leakage in closely spaced multiplexed arrays. The grating is a square-wave grating of 610 nm pitch, 50 nm depth and 11.9 μm in length, and, in the absence of the cantilever structure, is an efficient waveguide output coupler [14]. The bottom surface of the suspended cantilever is assumed to be a perfect reflector at the wavelength of

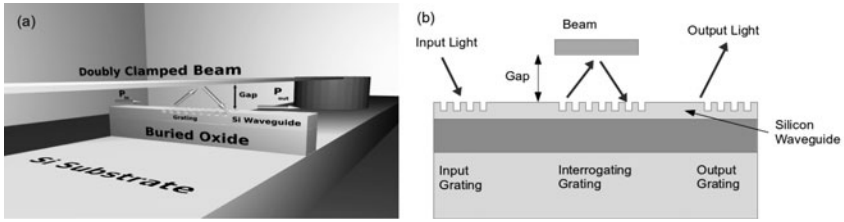

Fig. 1. (a) Isometric view of the proposed interrogating grating structure. (b) Cross-section of

interest (1550 nm), and extending 1 μm beyond the interrogating grating on all sides.

In the FDTD model, a TE polarized Gaussian beam at a wavelength of 1550 nm was launched into the waveguide. The diffraction grating was placed a sufficient distance away (8 μm) from the source so that a stable optical mode was incident on the grating section of the waveguide. The cross-section used for power simulations only contains the waveguide, so that substrate modes and small evanescent field contributions are not included in the power calculations.

Figure 2 shows the results of FDTD simulations of the fields present for different cantilever-grating separations. Figure 2(a) shows the optical TE field distribution through the device when the MEMS beam arm is at the height required to create constructive interference at a wavelength of 1550 nm. Figure 2(b) shows the TE distribution, when the MEMS beam is at the height required for destructive interference. When compared to Figure 2(a), it can be seen that for the case of Fig. 2(b), most of the light dissipates into the substrate. While not discussed here, this may provide an alternate detection method for this structure using a buried detector, substrate detector, or another grating waveguide structure. Discussion on the transmitted optical power as a function of the MEMS beam suspention height is delayed and until the Discussion section of this paper.

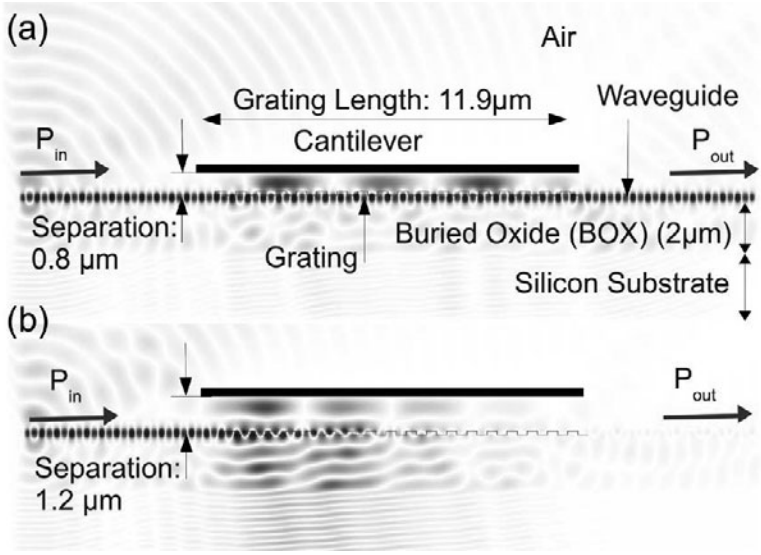

Fig. 2. Modeled results for the device formed using SOI structure and transmitting 1550 nm light below a perfectly reflecting MEMS beam. (a) Calculated TE field distributions for waveguide to beam separation of 0.8 μm. This separation gives maximum transmitted power. (b) TE field distribution with a separation 1.2 μm (minimum in transmitted power). A significant portion of the energy is coupled into the substrate rather than the output waveguide.

DEVICE FABRICATION AND EXPERIMENTAL SETUP

The waveguides and diffraction gratings were fabricated using a silicon on insulator (SOI) wafer by the LETI standard passive process using the ePIXfab silicon photonics platform. The buried oxide (BOX) layer was 2 µm thick, and the epitaxial silicon was 220 nm thick. The waveguides and gratings (pitch 630 nm, depth 70 nm) were etched into the silicon using a deep ultra-violet (DUV) lithography process. Silicon dioxide was then deposited to cover the structures and chemo-mechanically polished (CMP) down to a thickness of 100 nm above the waveguides in order to supply a flat surface for further fabrication steps.

Plasma enhanced chemical vapour deposition (PECVD) silicon nitride was used as the structural material to fabricate MEMS microbridges with a gold undercoat using surface micro-machining [16]. The gold was 50 nm thick in order to provide good reflection for the infra-red light that was used in the experiment. The beams were 220 µm long and 20 µm wide, with top hat style anchors. The sacrificial layer used was the low stress polyimide PI-2610 of thickness of 1.6 µm. The chip was bonded to a piezo-electric device which was used to drive the microbridge at its resonant frequency of 291 kHz. A Polytec OFV-5000 vibrometer controller with a DD-500 displacement decoder was used to monitor the displacement of the microbridges to determine the gap between the suspended beam and the waveguide and to measure the mechanical resonance frequency.

Fiber to fiber insertion losses were measured with an InGaAs photodetector to be 12-13 dB arising largely from the grating coupler losses. The amplitude change of this output power was then measured as a function of microbridge position above the central grating.

RESULTS AND ANALYSIS

Figure 3 shows the measured optical output at a wavelength of 1585 nm as a function of grating-microbridge gap for a piezo-driven MEMS beam over a 250 nm range at its resonant frequency of 291 kHz. The measured range was limited by the piezo drive power and not the beam characteristics. As the optical output results from an interferometric effect which is periodic with the gap under the beam, the optical output is not monotonic.

The measured transmitted optical power data shown in Fig. 3 are overlayed on optical

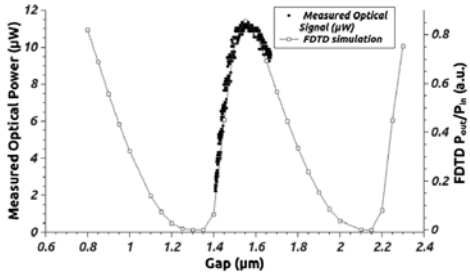

Fig. 3. Measured optical power transmitted through the device for several vibration cycles of the suspended microbridge (full circles) compared to 2D FDTD simulation results (open squares) as a function of the gap between the suspended MEMS beam and the underlying waveguide.

finite difference time domain (FDTD) simulations (open squares), which present the ratio of optical output power to input power as a function of the gap. The simulation data in Fig. 3 is for an optical transmitted signal of wavelength of 1585nm. Good correlation between the theoretical and experimental results is evident. Slight discrepancies between the model and the experimental results are most likely related to the assumed perfect reflector in the model, and the use of a 2D model which did not include optical fringing effects or mechanical dynamics at resonance.

CONCLUSIONS

An integrated readout technique for interrogating the suspension height of MEMS structures was presented. This readout technique is envisaged to be useful in applications such as MEMS-based biological and chemical sensing. The performance of the technique as predicted via FDTD simulations is confirmed by experimental measurements.

ACKNOWLEDGEMENTS

We acknowledge the support from the Australian Research Council, The Western Australian Node of the Australian National Fabrication Facility, and the Office of Science of the WA State Government.

REFERENCES

1. N. Lavrik, M. Sepaniak, and P. Datskos, “Cantilever transducers as a platform for chemical and biological sensors,” Rev. Sci. Instrum. 75, 2229-2253 (2004).
2. A. Loui, T. V. Ratto, T. S. Wilson, S. K. McCall, E.V. Mukerjee, A. H. Love, and B. R. Hart, “Chemical vapor discrimination using a compact and low-power array of piezoresistive microcantilevers,” *The Analyst*, vol. 133, no. 5, p. 608, 2008.
3. M. Baller, H. Lang, J. Fritz, C. Gerber, J. Gimzewski, U. Drechsler, H. Rothuizen, M. Despont, P. Vettiger, F. Battiston, J. Ramseyer, P. Fornaro, E. Meyer, and H. Guntherodt, “A cantilever array-based artificial nose,” Ultramicroscopy 82, 1-9 (2000).
4. Y. T. Yang, C. Callegari, X. L. Feng, K. L. Ekinci, andM. L. Roukes, “Zeptogram-Scale nanomechanical mass sensing,” Nano Lett., vol. 6, no. 4, pp. 583–586, Apr. 2006.
5. M. Li, H. X. Tang, and M. L. Roukes, “Ultra-sensitive NEMS-based cantilevers for sensing, scanned probe and very high-frequency applications,” Nature Nanotechnol., vol. 2, no. 2, pp. 114–120, Jan. 2007.
6. T. H. Stievater, W. S. Rabinovich, M. S. Ferraro, N. A. Papanicolaou, J. B. Boos, R. A. McGill, J. L. Stepnowski, and E. J. Houser, “Erratum: All-optical micromechanical chemical sensors [Appl. phys. lett. 89, 091125 (2006)],” Appl. Phys. Lett., vol. 89, no. 26, p. 269902, 2006.
7. D. Kong, T. Mei, Y. Tao, L. Ni, T. Zhang, W. Lu, Z. Zhang, and R. Wang, “A MEMS sensor array for explosive particle detection,” in Proc. Int. Conf. Inf. Acquisition, 2004, p. 278281.
8. T. Fukuma, M. Kimura, K. Kobayashi, K. Matsushige, and H. Yamada, “Development of low noise cantilever deflection sensor for multienvironment frequency-modulation atomic force microscopy,” Revi. Sci. Instrum., vol. 76, no. 5, p. 053704, 2005.

9. H. P. Lang,M. K. Baller, R. Berger, C. Gerber, J. K. Gimzewski, F.M. Battiston, P. Fornaro, J. P. Ramseyer, E. Meyer, and H. J. Gntherodt, “An artificial nose based on a micromechanical cantilever array,” Analytica Chimica Acta, vol. 393, no. 1–3, pp. 59–65, Jun. 1999.
10. C. Schonenberger and S. F. Alvarado, “A differential interferometer for force microscopy,” Revi. Sci. Instrum., vol. 60, no. 10, p. 31313134, 1989.
11. K. Zinoviev, C. Dominguez, J. A. Plaza, V. J. C. Busto, and L. M. Lechuga, “A novel optical waveguide microcantilever sensor for the detection of nanomechanical forces,” J. Lightw. Technol., 24, p. 2132, May 2006.
12. J. W. Noh, R. Anderson, S. Kim, J. Cardenas, and G. P. Nordin, “Inplane photonic transduction of silicon-on-insulator microcantilevers,” Opt. Exp., vol. 16, no. 16, pp. 12 114–12 123, 2008.
13. T. H. Stievater, W. S. Rabinovich, M. S. Ferraro, N. A. Papanicolaou, R. Bass, J. B. Boos, J. L. Stepnowski, and R. A. McGill, “Photonic microharp chemical sensors,” Opt. Exp., vol. 16, no. 4, pp. 2423–2430, Feb. 2008.
14. D. Taillaert, F. Van Laere, M. Ayre, W. Bogaerts, D. Van Thourhout, P. Bienstman, and R. Baets, “Grating couplers for coupling between optical fibers and nanophotonic waveguides,” Jpn. J. Appl. Phys., vol. 45, no. 8A, pp. 6071–6077, Aug. 2006.
15. A. F. Oskooi, D. Roundy, M. Ibanescu, P. Bermel, J. Joannopoulos, andS. G. Johnson, “Meep:Aflexible free-software package for electromagnetic simulations by the FDTD method,” Comput. Phys. Commun., vol. 181, no. 3, pp. 687–702, Mar. 2010.
16. M. Martyniuk, J. Antoszewski, C. A. Musca, J. M. Dell, and L. Faraone, “Stress in low-temperature plasma enhanced chemical vapour deposited silicon nitride thin films,” Smart Materials and Structures, vol. 15, no. 1, pp. S29–S38, Feb. 2006.